Inelastic neutron scattering study of the H2 interaction with carbon-supported Pt and Pd catalysts

Inelastic neutron scattering study of the H_2 interaction with carbon-supported Pt and Pd catalysts

Eleonora Vottero[a]*, Michele Carosso[a], Riccardo Pellegrini[b], Mónica Jiménez-Ruiz[c], Elena Groppo[a] and Andrea Piovano[c]

a) Department of Chemistry, NIS Centre and INSTM, University of Turin, Via G. Quarello15/A, Turin, I-10135, Italy
b) Chimet SpA-Catalyst Division, Via di Pescaiola 74,Viciomaggio Arezzo, I-52041, Italy
c) Institut Laue-Langevin(ILL),71 Avenue des Martyrs, CS 20156, 38042 Grenoble Cedex 9, France

*eleonora.vottero@unito.it

Abstract

Carbon-supported Pt and Pd catalysts are largely employed as heterogeneous catalysts for hydrogenation reactions. Albeit their routine use in industry, many details about their interaction with H_2 are still not completely understood. In this article, we propose a detailed investigation of the behavior in the presence of H_2 of an activated carbon and of two catalysts obtained by depositing on it Pt and Pd nanoparticles by means of Inelastic Neutron Scattering (INS) spectroscopy. The high-quality INS spectra of the three samples were measured in absence and in presence of different amounts of H_2, providing very detailed information about H_2 physisorption on each system and about the nature of the metal hydrides formed upon hydrogenation of the catalysts. In addition, we were also able to obtain a direct observation of the occurrence of hydrogen spillover from the metal nanoparticles onto the activated carbon, as revealed by the increase of the number of C-H species at the borders of the graphenic domains. Overall, this work provides important insights for better understanding the complex nature of the interaction between H_2 and Pt and Pd-loaded activated carbon catalysts.

Keywords

INS spectroscopy, activated carbon, platinum nanoparticle, palladium nanoparticle, metal hydride, hydrogen spillover

Graphical abstract

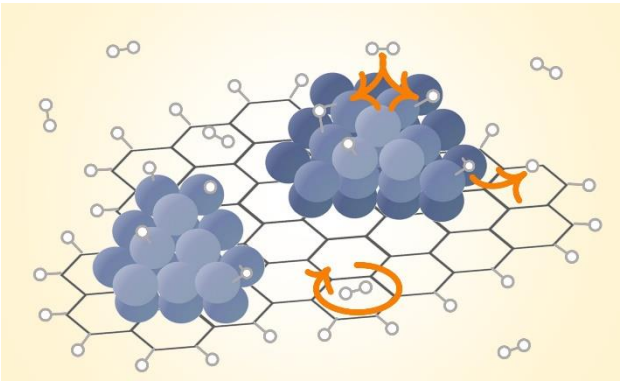

1. Introduction

Pt and Pd nanoparticles on carbonaceous supports are widely employed as heterogeneous catalysts for hydrogenation reactions. They find application in fundamental industrial sectors such as fine chemistry, pharmaceutical or food industry, or as fuel cell electrocatalysts [1-3]. Carbonaceous materials are also largely investigated as hydrogen storage materials, and the introduction of metal nanoparticles was demonstrated to be able to increase the hydrogen uptake of the material [4, 5]. For all these applications, a better understanding of the interaction between H_2 and carbon-based materials loaded with metal nanoparticles is of pivotal importance.

There are three main ways hydrogen can interact with this kind of composite materials. The first one consists in the physisorption of molecular H_2 on the carbon surface: the process is favored by the very large surface area of these materials but, on the other hand, H_2 uptake on pure carbonaceous materials is usually quite modest due to the weak interaction between the H_2 molecule and the aromatic domains [6]. The second way involves the metal nanoparticles, and relies on their ability to split molecular hydrogen and form metal hydrides. Pt is known to form superficial Pt hydrides with linear, two-fold and three-fold coordination, and small Pt nanoparticles were shown to undergo significant reconstruction processes as a function of the temperature and of the H_2 partial pressure [7, 8]. Pd, on the other hand, has the tendency to form bulk hydride phases in which H occupies the octahedral interstices in the fcc lattice of the metal. Two distinct phases, α and β, were identified and, at 25°C, they are observed at a H/Pd ratio lower or equal to 0.017 and higher than 0.60, respectively [9]. At intermediate stoichiometries, a mixture of the two phases is observed. Nanosized Pd particles exhibit a similar yet distinct behavior, characterized by a narrower miscibility gap and a decreased hysteresis between H_2 adsorption and desorption [10-12]. Furthermore, modifications in the sub-surface region of the Pd nanoparticles with the possible occupation of tetrahedral interstices [13, 14], as well as the formation of surface Pd-H species [14, 15], become relevant phenomena in highly dispersed nanoparticles. A complete understanding of the amount and nature of the metal hydrides formed is fundamental for both catalysis and hydrogen storage applications, since the M-H species are those involved in the hydrogenation reaction and they can significantly increase the H_2-uptake of the sample.

Finally, the third possible way H_2 can interact with metal nanoparticles loaded activated carbons is the so-called spillover process. This phenomenon consists of the migration of H atoms generated by the splitting of H_2 at the surface of the metal nanoparticles onto the underlying support [5, 16]. The form in which the spiltover H atoms can interact with carbon-based supports has been under debate for a long time. The possible migration of H onto perfect graphenic planes has been largely investigated, but it does not appear to be energetically favored [17-19]. In contrast, in recent years, several studies indicated that terminations of the aromatic domains, defects, heteroatoms, or dopants are fundamental in enhancing the spillover process over carbonaceous materials [5, 20, 21].

Among the available characterization techniques, Inelastic Neutron Scattering (INS) spectroscopy has the great advantage to be very sensitive to the signal arising from the H-containing species in the sample [22]. When dealing with metal nanoparticles supported on carbonaceous materials in the presence of H_2, it allows to simultaneously observe the signals of the rotational transitions of free and physisorbed H_2, as well as the vibrational transitions of H bonded on the activated carbon and on the metal nanoparticles in the form of hydrides [15, 23-30]. In this work, we report the results obtained by measuring the INS spectra in the presence of H_2 of an activated carbon obtained via physical activation of a wood precursor with steam, and of two catalysts obtained by depositing highly dispersed Pt and Pd nanoparticles on said support at the relatively modest metal loading of 5 w/w%. For comparison, also the spectra obtained for similar Pt/Al_2O_3 and Pd/Al_2O_3 samples will be shown and discussed. These same samples were already widely investigated by employing multiple techniques in the past [31-36], and in the current work we aim to present the full potential of modern INS spectrometers in measuring very subtle spectral modifications, providing important insights about the differences in H_2 physisorption, metal hydrides formation and H-spillover in activated carbon-supported catalysts.

2. Experimental and methods

2.1. Samples and preparation

The samples described in this work were provided and prepared by the company Chimet S.p.A. The alumina-based samples are supported on a transition alumina (SSA = 116 m^2g^{-1}; pore volume = 0.41 cm^3g^{-1}) hereinafter referred to as Al_2O_3. For the activated carbon-based samples, instead, a physically activated carbon of wood origin (SSA = 1018 m^2g^{-1}, pore volume = 0.63 cm^3g^{-1}) was employed as the support, hereinafter referred to as CwA. The Pd-containing samples were prepared following the deposition-precipitation method described in [37, 38], by using Na_2PdCl_4 as the metal precursor and Na_2CO_3 as the basic agent. Analogously, the Pt-containing samples were prepared by a deposition-precipitation method similar to the one described in [39]. Samples Pd/Al_2O_3 and Pd/CwA were pre-reduced in a HCOONa solution at 55°C for 1 h, Pt/CwA was pre-reduced with the same solution at 80°C, while Pt/Al_2O_3 was not pre-reduced after the preparation. Finally, all samples were carefully washed with distilled water to remove all the residual Cl, and then dried overnight at 120°C. The labels used for each sample and their main features are summarized in Table 1.

Table 1: Summary of catalysts investigated in the present work and of their main features: support, metal loading, and metal dispersion evaluated by means of CO chemisorption.

Label	Support	Metal	Dispersion
Pt/CwA	Activated carbon	Pt (5w/w%)	72 %
Pd/CwA	Activated carbon	Pd (5w/w%)	24 %
Pt/Al_2O_3	Al_2O_3	Pt (5w/w%)	80 %
Pd/Al_2O_3	Al_2O_3	Pd (5w/w%)	24 %

2.2. INS measurements

The INS spectra were measured on the instrument IN1/Lagrange at the ILL in Grenoble (France) [40-42]. The spectra were collected from 24 to 2000 cm^{-1} with a resolution $\Delta E/E$ = 2%. Prior to each measurement, an amount of sample comprehended between 1.6 and 2.4 g was outgassed at a temperature of 393 K to remove all physisorbed water and, in the case of the metal-containing catalysts, reduced by sending 100 mbar of H_2 for three times at 393 K and then further outgassed at the same temperature. All the following sample handling was performed within a glovebox to avoid the re-adsorption of water vapor. The samples were then inserted within cylindrical Al cells (height = 4 cm; diameter = 16 mm), sealed with In wire, mounted on a gas injection stick and connected to a gas dosing device. For all the experiments, the sample was at first measured as such under vacuum, and then after dosing H_2 up to the desired equilibrium pressure. H_2 dosing was performed at room temperature, and then the sample was cooled to 24 K for the whole duration of the measurement by employing a CCR (closed cycle refrigerator) cryostat. The details of all the experiments are summarized in Table 2. The spectra were measured by using the Si(111), Si(311) and Cu(220) monochromators, and the obtained spectral ranges were merged by using the procedure described in [31]. The difference spectra shown in sections 3.2 and 3.3 were calculated over spectra re-binned over three or five consecutive points to reduce the noise level of the signal.

Table 2: Summary of the measurement conditions employed for the experiments herein discussed.

Measurement	Sample	Temperature of the INS measurement (K)	Equilibrium H_2 pressure (mbar)
1	CwA	24 K	0
1a			230
1b			450
2	Pt/CwA	24 K	0
2a			230
2b			420
3	Pd/CwA	24 K	0
3a			230
3b			430
4	Pt/Al_2O_3	24 K	0
4a			130
5	Pd/Al_2O_3	24K	0
5a			430

3. Results and discussions

3.1. H_2-physisorption

The INS spectra of CwA measured under vacuum and in the presence of 230 and then 450 mbar of H_2 are reported Figure 1A. The main signals present in the spectrum of bare CwA are observed in the 750-1000 cm^{-1} spectral range, corresponding to the out-of-plane bending modes of the C-H terminations in the graphenic domains, and in the 1000-1600 cm^{-1} region, which is associated with the in-plane bending modes of said terminations. Furthermore, the signals in the 400-700 cm^{-1} spectral range are attributed to the so-called riding modes, i.e. deformation modes of the carbon skeleton enhanced by the displacement of H atoms bonded to it [32, 43]. The region of the bending modes is the most informative one and is diagnostic of the amount of C-H terminations in the activated carbon sample and of the morphology of the graphenic domains [32, 44]. The INS spectra of Pt/CwA and Pd/CwA (Figure 1B and C) exhibit very similar profiles to the one of CwA, and mostly differ for a slight decrease in intensity of the signals in the 750-1000 and 1000-1600 cm^{-1} ranges. This decrease was attributed to the interaction between the metal nanoparticles and the terminal C-H groups of the aromatic domains, and is commented more in detail in reference [32].

When dosing H_2, CwA is able to physisorb relevant amounts of gas. This phenomenon results in a significant modification of the INS spectra, highlighted in the difference spectra in Figure 1A', B' and C'. More in detail, the new sharp signal at 120 cm^{-1} is due to the J(1←0) rotational transition of H_2, while the broader signals centered around 260 and 1430 cm^{-1} are assigned to the J(1←0) and J(3←0) rotational transitions shifted by the recoil energy [31, 45-47]. The differential spectra for Pt/CwA are very similar to those of CwA (Figure 1B'), while for Pd/CwA the intensity of the signal attributed to physisorbed H_2 is much weaker (Figure 1C'). Additional weak signals appear in the Pt/CwA and Pd/CwA differential spectra upon H_2 dosing, and are related to the formation of other hydrogenous species following the interaction of H_2 with the metal nanoparticles, as it will be discussed in further detail in sections 3.2 and 3.3.

More detailed information on H_2 physisorption in the three samples can be retrieved by taking a closer look at the J(1←0) rotational transition at 120 cm^{-1}. For this purpose, the magnification of said signal for CwA, Pt/CwA and Pd/CwA at the highest H_2 equilibrium pressure is reported in Figure 2. Three components centered at 107, 120 and 132 cm^{-1} are clearly visible: the central peak is associated with the

J(1←0) rotational transition of the free H_2 molecule, while the peripheral signals are due to the perturbation of said signal upon physisorption of the H_2 molecules on the support. The signal splitting is due to the loss of degeneracy between the (J=1, M=0) and (J=1, M= ±1) energy states, and the observed 2:1 intensity ratio between the 107 and the 132 cm^{-1} peaks indicates that the H_2 molecules are adsorbed side-on onto the carbon support [31, 46]. The spectra of the H_2 rotor is very similar for CwA and Pt/CwA, and they mostly differ for the broader profile of the side peaks in the latter case. This observation, commented more in detail in ref [31], has been interpreted in terms of two additional and weak signals at about 90 and 150 cm^{-1}, which have been attributed to molecular H_2 physisorbed on the hydrogenated Pt nanoparticles. The nature of the H_2 rotor signal is instead quite different for the Pd/CwA shown in Figure 2C. Albeit all three samples underwent H_2 dosing at room temperature up to comparable equilibrium pressure and were then cooled to 24 K for the INS measurements, Pd/CwA was the only sample to present such weak signals corresponding to the rotor of molecular H_2 in its spectrum. The profile of the signal is also clearly different: in this case, the central peak at 120 cm^{-1} is by far the most intense one, while the satellite peaks at 107 and 132 cm^{-1} are barely visible. These observations, together with the weak recoil profile (Figure 1C') indicate that less gaseous H_2 was present in the cell, and also that very little H_2 was physisorbed on the activated carbon surface. This suggests that the H_2 dosed at room temperature was converted into other species upon the cooling of the sample preceding the measurement. Considering that Pd was observed to absorb larger amounts of H_2 at low temperature [48], we hypothesize that the amount of molecular H_2 in the cell decreased when cooling the sample in favor of the formation of Pd hydride species.

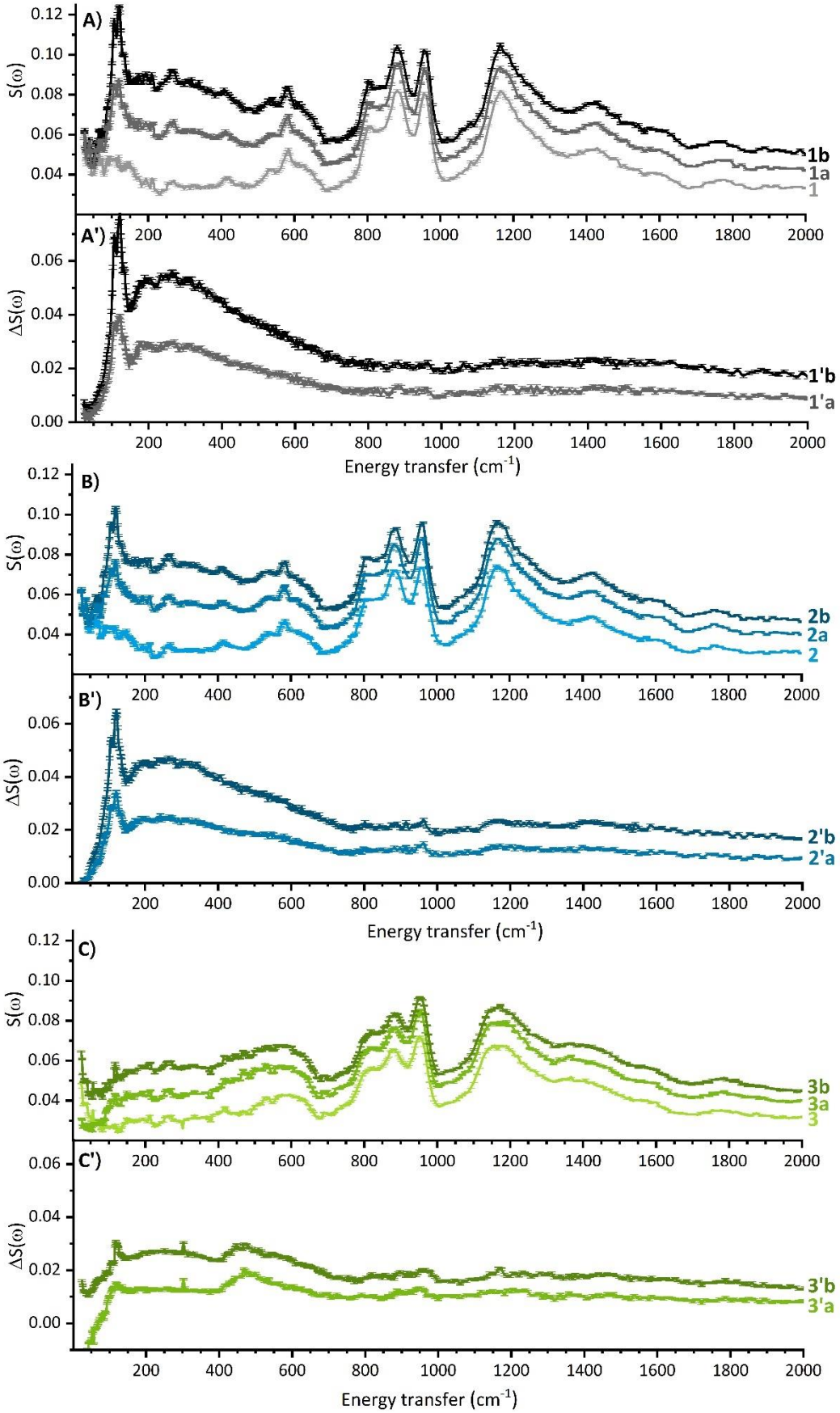

Figure 1: INS spectra of CwA (A), Pt/CwA (B) and Pd/CwA (C) measured in vacuum and in the presence of two H_2 equilibrium pressures. The spectral contributions corresponding to the H_2 rotor on CwA were obtained by calculating the differences 1a – 1 = 1'a and 1b – a = 1'b, and are shown in part A'. The analogous differences calculated for Pt/CwA and Pd/CwA are shown in panels B' and C', respectively.

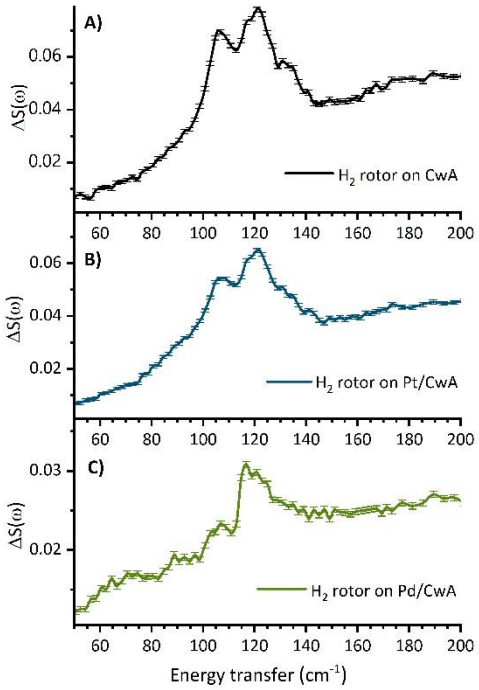

Figure 2: Detail over the J(1←0) rotational transition for CwA (A), Pt/CwA (B) and Pd/CwA (C). Notice that part C was plotted on a y range three times smaller than in parts A and B.

3.2. Metal hydrides formation

Pt and Pd are very active metals for splitting H_2, resulting in the formation of superficial and/or bulk metal hydride species detectable by INS. In the case of activated carbon-supported samples, the analysis of the INS spectral profiles of said species is hampered by the overlapping signals of physisorbed H_2 (as discussed in section 3.1) and spiltover species. To easily describe and isolate the spectral features of Pt-H and Pd-H alone, we thus decided to start our analysis from the simpler Pt/Al_2O_3 and Pd/Al_2O_3 samples, whose INS spectra under vacuum and in the presence of H_2 are shown in Figure 3A and B. The spectra of the two samples measured under vacuum are the same, and are characterized by a very broad signal centered around 900 cm^{-1} which is ascribed to bending and deformation modes of -OH groups at the surface of alumina [49, 50]. This support presents a much lower surface area than the activated carbon one and, consequently, the spectral profile of physisorbed H_2 was not observed in this case. Also, no modifications to the spectral features of the surface -OH groups are observed, indicating that no H-spillover occurred under these experimental conditions. Generally speaking Al_2O_3, being a non-reducible support, is not prone to relevant H-spillover [51]. In our experience, we were only able to observe a very small increase of the INS signal of -OH groups on a highly dehydroxylated Pt/Al_2O_3 sample, obtained by pre-treating the sample by outgassing at 573 K. Thus, the only possible contributions to the difference spectra calculated in Figure 3A' and B' correspond to Pt-H and PdH species, respectively.

More in detail, the complex profile in Figure 3A' corresponds to the bending modes of surface Pt-H species (350-750 cm^{-1}) and to the stretching modes of multi-folded Pt-H species (800-1600 cm^{-1}). The full data analysis, discussed in more detail in ref [49], also pointed out a strong dependence of this spectral profile on the hydrogenation conditions (i.e. the temperature and the H_2 equilibrium pressure). In this respect, the comparison between experimental and simulated spectra confirmed that the employed conditions lead to a very high degree of H-coverage, and that under said conditions the Pt nanoparticles reconstruct into cuboctahedric or disordered morphologies in which the interaction between the nanoparticle and the support is weakened in favor of the formation of new Pt-H bonds. The difference spectrum calculated for sample Pd/Al_2O_3 and shown in Figure 3B' presents a large and asymmetric peak centered at 463 cm^{-1},

corresponding to the vibrational modes of the β-PdH phase. The weaker signal above 850 cm^{-1} is instead associated with the first overtone of said modes [23, 52]. The presence of some residual α-PdH phase, identifiable by a signal at about 555 cm^{-1} [15, 53] or of Pd-H species at the surface [15, 54-57] cannot be completely ruled out as their signals would be subsided to the broad and more intense signal of the β-PdH phase.

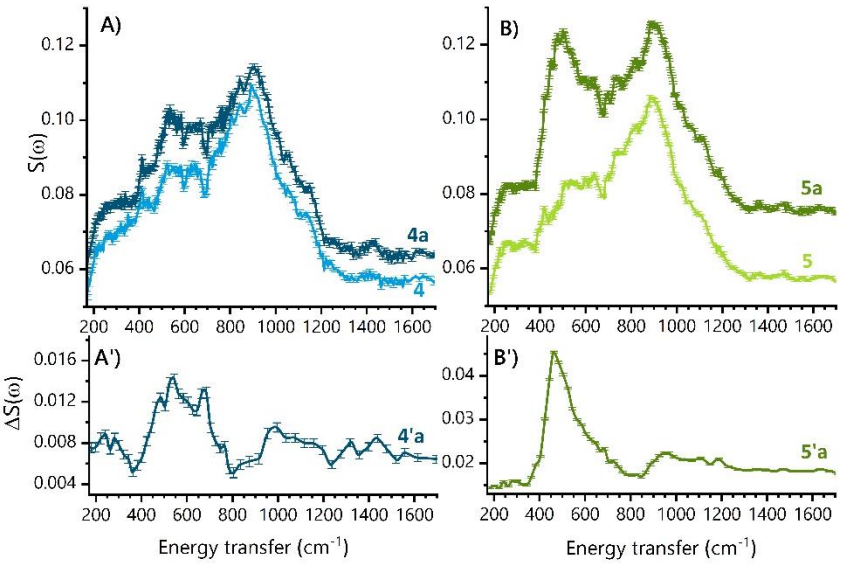

Figure 3: INS spectra of Pt/Al_2O_3 and Pd/Al_2O_3 (A and B, respectively) measured under vacuum and in the presence of H_2. The difference spectra, containing the INS profile relative to the new species formed in H_2 atmosphere, are reported in A 'and B'.

The spectra of the hydrogenous species formed upon interaction of Pt/CwA and Pd/CwA with H_2 are shown in Figure 4A', A", B' and B". In this case, the simple difference between the spectra measured in hydrogen and the spectra of the bare samples under vacuum are still dominated by the recoil profile of physisorbed H_2, hindering a clear interpretation (see spectra 2a', 2b', 3a' and 3b' in Figure 1). Thus, we further subtracted the contribution of physisorbed molecular H_2 (spectra 1'a and 1'b in Figure 1) after normalization to the H_2 amount, in order to isolate the spectral profile of the sole new H-containing species formed in the samples. The double differential spectra calculated for Pt/CwA are reported in Figure 4A' and A". To ease the comparison, the spectrum of the Pt-H species obtained for the Pt/Al_2O_3 sample (spectrum 4'a in Figure 3) is also shown. Albeit the very weak intensity of the signals, a remarkable resemblance between these spectra is clearly observed in the 400-700 cm^{-1} region. The matching of this signal in the two experiments both in terms of position and of the spectral profile strongly suggests that the hydrogenated Pt nanoparticles present a cuboctahedric morphology also in Pt/CwA. Analogously to what observed for the Pt/Al_2O_3 sample under similar conditions [49], the Pt nanoparticles in the presence of H_2 would thus be characterized by a weak degree of interaction with the support in favor of the complete solvation by the adsorbate. In the 800-1600 cm^{-1} region, instead, where the corresponding stretching modes of the multi-folded Pt-H species would be expected, the differential spectra of Pt/CwA and Pt/Al_2O_3 in the presence of H_2 are clearly different due to the prevalence of new bands in the former case, as will be discussed in more details in section 3.3.

The same comparison for the Pd-based catalysts is shown in Figure 4B' and B". The differential spectrum for Pd/CwA is characterized by a main peak centered around 465 cm^{-1}, which strongly resembles the signal of the β-PdH phase already observed for Pd/Al_2O_3 (Figure 3B'). Also for the Pd/CwA measurements, further signals are present in the 800-1600 cm^{-1} spectral range and will be discussed in section 3.3. The two spectra obtained for experiments 3a and 3b are quite similar, apart from a much more pronounced signal between 550 and 700 cm^{-1} observed for experiment 3b (Figure 4B"). This signal, neither observed in the Pd/Al_2O_3 sample nor at lower amounts of H_2, is too intense to be attributed to the asymmetric broadening of the β-PdH signal and is likely to be associated with other Pd-H vibrations. A similar change in intensity at about 660 cm^{-1} was observed in the past by Albers *et al* after consecutive cycles of H_2 absorption and

desorption on a 20% Pd/C sample [23]. The authors attributed the presence of this signal to sub-surface Pd-H species, and they interpreted its decrease in terms of a reduction of said sites due to a lattice relaxation favored by the consecutive H_2 absorption-desorption cycles. Indeed, the formation of sub-surface hydride species in Pd nanoparticles has been widely reported, and the formation of hydrides in both octahedral and tetrahedral interstices was observed [13, 25, 58]. According to previous studies, H atoms in tetrahedral interstices may contribute to the signal observed at about 980-1000 cm^{-1} [25, 59], while H in octahedral interstices are a more plausible assignment for the 600 cm^{-1} shoulder [29, 60]. The population of surface Pd-H sites upon larger H_2 pressure can also be hypothesized. In particular, past HREELS studies reported two vibrational modes of H bonded on the Pd(100) surface at 507 and 612 cm^{-1} [56, 57], while signals at 773 and 999 cm^{-1} were observed for H chemisorbed on the Pd(111) surface [54].

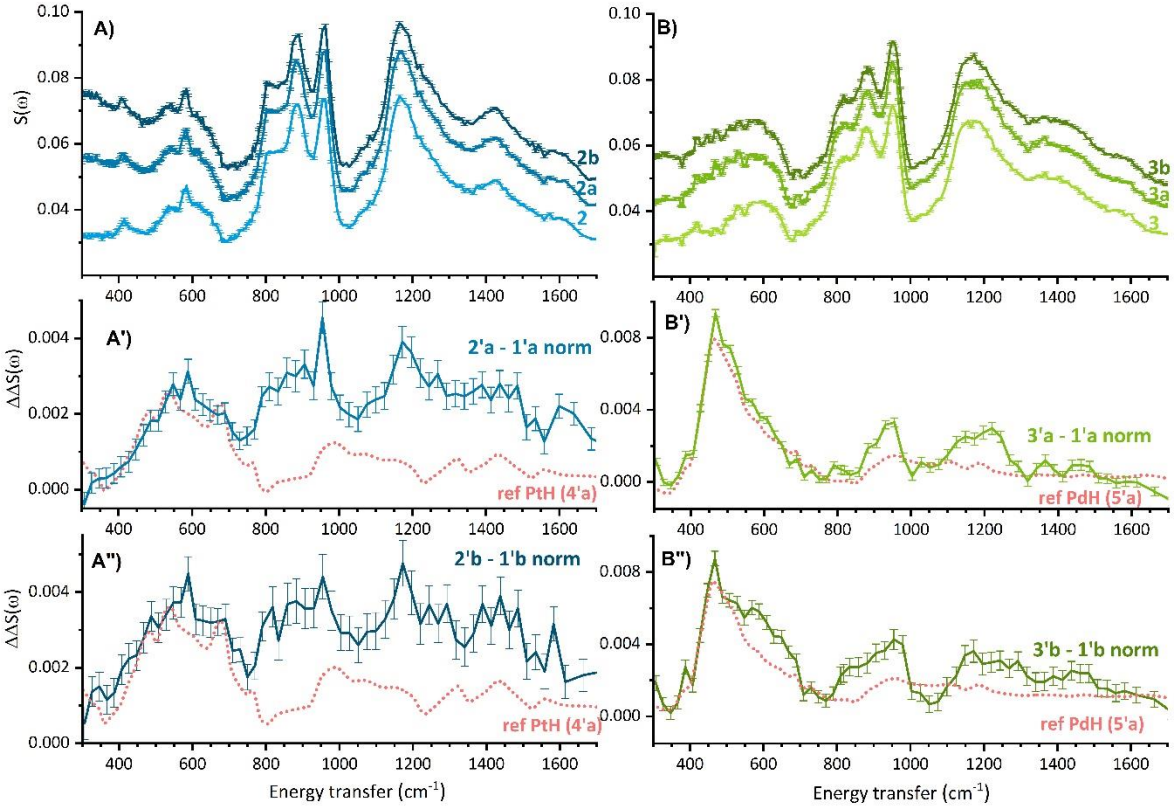

Figure 4: INS spectra of Pt/CwA and Pd/CwA as such and in the presence of two increasing H_2 equilibrium pressures (panels A and B, respectively). The profile of the hydrogenous species formed upon interaction of the samples with H_2 were obtained by subtracting the spectra of the catalyst as such to the one in H_2 and by further subtracting the contribution of molecular H_2 shown in Figure 1A', resulting in the double differential spectra shown in parts A', A", B' and B". The spectral profiles of Pt-H and Pd-H species obtained for the Al_2O_3-supported samples are shown as a reference, and were normalized and shifted vertically for clarity.

3.3. H-spillover onto the carbon support

In all the differential INS spectra of the Pt/CwA and Pd/CwA samples measured in the presence of H_2, it is possible to observe the formation of two sets of signals in the 800-1000 and 1000-1600 cm^{-1} ranges (see Figure 4A', A", B' and B"). These changes were instead not observed in the case of the sole CwA support (Figure 1A'). On a closer inspection, it is possible to notice that the maxima position of said peaks corresponds to the C-H bending signals in the original spectra (spectra 2 and 3 in Figure 4). This indicates a slight increase in the amount of the C-H terminations of the activated carbon following the migration of H atoms from the metal nanoparticles onto the support, and it is a direct observation of H-spillover. It is also worth noticing that the signal observed are typical of C-H terminations of aromatic domains in which the C hybridization is sp^2, meaning that the spillover process we observed does not cause a change in the hybridization state of the C atoms involved. The fact that the phenomenon is only observed for the supported Pt and Pd samples also

confirms that, under these experimental conditions, an active phase able to split the H_2 molecule is required to observe a sensible amount of chemisorbed H on the carbon support [4, 5]. In the past this phenomenon was already observed by INS on similar catalysts [15, 23, 26] but, to our knowledge, this is the first time it is reported so clearly on samples with a modest metal loading of 5 w/w%.

It is generally assumed that a few unsaturated border sites along the aromatic platelets are the ones being hydrogenated following the H-spillover process [15, 23]. Considering that we previously observed a slight decrease in the amount of C-H terminations upon the metal nanoparticles deposition (as evident when comparing spectra 1, 2 and 3 Figure 1, and better discussed in references [31, 32]), it is plausible that the H-spillover phenomenon observed in this experiment corresponds to a restoration of part of said terminations.

A precise quantification of the splitover H onto the carbon support for the two samples is hindered by the overlapping with some weaker signals relative to the metal hydride species, already commented in section 3.2, but some qualitative considerations can be done. In the case of the Pt/CwA sample, within the measurement error, the amount of new C-H terminations formed upon H-spillover seems similar between measurements 2a and 2b (Figure 4A' and A"), meaning that the spillover process was likely to be completed already after dosing H_2 for the first time. In the case of Pd/CwA instead, a significant increase of the signals related to terminal C-H species is observed between measures 3a and 3b (Figure 4B' and B"). As already commented in section 3.1, the formation of bulk Pd-H species is the dominating process during measure 3a, while further dosing of H_2 in measure 3b resulted in a small amount of physisorbed H_2 and in an increase of H-spillover onto the support.

4. Conclusions

In this work, we present our investigation of the interaction of H_2 with an activated carbon and two catalysts obtained by depositing Pt and Pd nanoparticles on it, by focusing on the information obtained by means of INS spectroscopy. We were able to analyse the physisorption process of molecular H_2 by comparing the characteristic signal for the J(1←0) rotational transition on the three samples. CwA and Pt/CwA exhibit similar features, typical of H_2 molecules physisorbed side-on onto the carbon support. In addition, Pt/CwA presents some additional and weak signals attributed to H_2 physisorbed on the hydrogenated Pt nanoparticles [31]. The Pd/CwA sample instead presented a significantly different spectral profile, characterized by very weak bands corresponding to physisorbed H_2. Considering that all three samples were brought to comparable H_2 equilibrium pressure upon dosing H_2 at room temperature, and that Pd was shown to absorb a larger amount of hydrogen at a lower temperature, we attribute this behavior to an enrichment of the Pd-H phase while cooling the sample down to 24 K performed before starting the measurement.

Following, we focused our attention on the metal hydride species formed in the Pt/CwA and Pd/CwA samples. In the former case, the spectral profile corresponding to the vibrational modes of Pt_xH_y nanoparticles in cuboctahedric or disordered morphology and in weak interaction with the support was observed. In analogy to what was previously observed on a Pt/Al_2O_3 sample, this morphology may be attributed to the reconstruction of the supported Pt nanoparticles upon increasing the H_2 equilibrium pressure of the system [49]. For the Pd/CwA sample instead, the typical signals of the β-PdH phase can be observed in both the experiments, and under a higher H_2 loading a new signal ascribable to subsurface and surface PdH species also arises.

Finally, signals assigned to H-spillover were observed on both Pt/CwA and Pd/CwA. The occurrence of the phenomenon is evinced by the intensification of the typical signal corresponding to the bending modes of the C-H terminations of the activated carbon support. So that a decrease of these C-H terminations was observed following the deposition of the metal nanoparticles onto the support, we hypothesize that the H-spillover herein observed consisted in the restoration of part of said terminations. Furthermore, the observed spectral features indicate that the C atom involved did not undergo any change of hybridization, as the formed bands are typical of C-H terminations in aromatic structures in which the hybridization state of C is sp^2. In the case of Pt/CwA the spillover process seems to be completed already after the first H_2 dosing, while

in the case of Pd/CwA the formation of PdH species was the dominant phenomenon during the first dosing and a significant increase in splitover H and physisorbed H_2 were observed following the second H_2 dosing.

Overall, these findings are important to better understand the real behavior of these catalysts under hydrogenation conditions, and the forms in which they are able to store hydrogen.

References

[1] E. Auer, A. Freund, J. Pietsch, T. Tacke, Carbons as supports for industrial precious metal catalysts, Applied Catalysis A: General, 173 (1998) 259-271.

[2] F. Maillard, P.A. Simonov, E.R. Savinova, Carbon Materials as Supports for Fuel Cell Electrocatalysts, Carbon Materials for Catalysis2008, pp. 429-480.

[3] V. Arunajatesan, B. Chen, K. Möbus, D.J. Ostgard, T. Tacke, D. Wolf, Carbon-Supported Catalysts for the Chemical Industry, Carbon Materials for Catalysis2008, pp. 535-572.

[4] Y. Li, R.T. Yang, Hydrogen Storage on Platinum Nanoparticles Doped on Superactivated Carbon, The Journal of Physical Chemistry C, 111 (2007) 11086-11094.

[5] D.S. Pyle, E.M. Gray, C.J. Webb, Hydrogen storage in carbon nanostructures via spillover, International Journal of Hydrogen Energy, 41 (2016) 19098-19113.

[6] P. Bénard, R. Chahine, Storage of hydrogen by physisorption on carbon and nanostructured materials, Scripta Materialia, 56 (2007) 803-808.

[7] L.-L. Wang, D.D. Johnson, Shear Instabilities in Metallic Nanoparticles: Hydrogen-Stabilized Structure of Pt37 on Carbon, Journal of the American Chemical Society, 129 (2007) 3658-3664.

[8] C. Mager-Maury, G. Bonnard, C. Chizallet, P. Sautet, P. Raybaud, H2-Induced Reconstruction of Supported Pt Clusters: Metal–Support Interaction versus Surface Hydride, ChemCatChem, 3 (2011) 200-207.

[9] F.D. Manchester, A. San-Martin, J.M. Pitre, The H-Pd (hydrogen-palladium) System, Journal of Phase Equilibria, 15 (1994) 62-83.

[10] A. Pundt, M. Suleiman, C. Bähtz, M.T. Reetz, R. Kirchheim, N.M. Jisrawi, Hydrogen and Pd-clusters, Materials Science and Engineering: B, 108 (2004) 19-23.

[11] S. Kishore, J.A. Nelson, J.H. Adair, P.C. Eklund, Hydrogen storage in spherical and platelet palladium nanoparticles, Journal of Alloys and Compounds, 389 (2005) 234-242.

[12] M. Yamauchi, R. Ikeda, H. Kitagawa, M. Takata, Nanosize Effects on Hydrogen Storage in Palladium, The Journal of Physical Chemistry C, 112 (2008) 3294-3299.

[13] H. Akiba, M. Kofu, H. Kobayashi, H. Kitagawa, K. Ikeda, T. Otomo, O. Yamamuro, Nanometer-Size Effect on Hydrogen Sites in Palladium Lattice, Journal of the American Chemical Society, 138 (2016) 10238-10243.

[14] C. Chizallet, G. Bonnard, E. Krebs, L. Bisson, C. Thomazeau, P. Raybaud, Thermodynamic Stability of Buta-1,3-diene and But-1-ene on Pd(111) and (100) Surfaces under H2 Pressure: A DFT Study, The Journal of Physical Chemistry C, 115 (2011) 12135-12149.

[15] S.F. Parker, H.C. Walker, S.K. Callear, E. Grünewald, T. Petzold, D. Wolf, K. Möbus, J. Adam, S.D. Wieland, M. Jiménez-Ruiz, P.W. Albers, The effect of particle size, morphology and support on the formation of palladium hydride in commercial catalysts, Chemical Science, 10 (2019) 480-489.

[16] W.C. Conner, J.L. Falconer, Spillover in Heterogeneous Catalysis, Chemical Reviews, 95 (1995) 759-788.

[17] G.M. Psofogiannakis, G.E. Froudakis, DFT Study of the Hydrogen Spillover Mechanism on Pt-Doped Graphite, The Journal of Physical Chemistry C, 113 (2009) 14908-14915.

[18] A. Sihag, Z.-L. Xie, H.V. Thang, C.-L. Kuo, F.-G. Tseng, M.S. Dyer, H.-Y.T. Chen, DFT Insights into Comparative Hydrogen Adsorption and Hydrogen Spillover Mechanisms of Pt4/Graphene and Pt4/Anatase (101) Surfaces, The Journal of Physical Chemistry C, 123 (2019) 25618-25627.

[19] M. Blanco-Rey, J.I. Juaristi, M. Alducin, M.J. López, J.A. Alonso, Is Spillover Relevant for Hydrogen Adsorption and Storage in Porous Carbons Doped with Palladium Nanoparticles?, The Journal of Physical Chemistry C, 120 (2016) 17357-17364.

[20] Z. Wang, F.H. Yang, R.T. Yang, Enhanced Hydrogen Spillover on Carbon Surfaces Modified by Oxygen Plasma, The Journal of Physical Chemistry C, 114 (2010) 1601-1609.

[21] V.B. Parambhath, R. Nagar, K. Sethupathi, S. Ramaprabhu, Investigation of Spillover Mechanism in Palladium Decorated Hydrogen Exfoliated Functionalized Graphene, The Journal of Physical Chemistry C, 115 (2011) 15679-15685.
[22] S.F. Parker, A.J. Ramirez-Cuesta, J. Tomkinson, Vibrational spectroscopy with neutrons: With applications in chemistry, biology, materials science and catalysis, 2005.
[23] P.W. Albers, J.G.E. Krauter, D.K. Ross, R.G. Heidenreich, K. Köhler, S.F. Parker, Identification of Surface States on Finely Divided Supported Palladium Catalysts by Means of Inelastic Incoherent Neutron Scattering, Langmuir, 20 (2004) 8254-8260.
[24] P.C.H. Mitchell, A.J. Ramirez-Cuesta, S.F. Parker, J. Tomkinson, D. Thompsett, Hydrogen Spillover on Carbon-Supported Metal Catalysts Studied by Inelastic Neutron Scattering. Surface Vibrational States and Hydrogen Riding Modes, The Journal of Physical Chemistry B, 107 (2003) 6838-6845.
[25] M. Kofu, N. Hashimoto, H. Akiba, H. Kobayashi, H. Kitagawa, K. Iida, M. Nakamura, O. Yamamuro, Vibrational states of atomic hydrogen in bulk and nanocrystalline palladium studied by neutron spectroscopy, Physical Review B, 96 (2017) 054304.
[26] C.I. Contescu, C.M. Brown, Y. Liu, V.V. Bhat, N.C. Gallego, Detection of Hydrogen Spillover in Palladium-Modified Activated Carbon Fibers during Hydrogen Adsorption, The Journal of Physical Chemistry C, 113 (2009) 5886-5890.
[27] C.-S. Tsao, Y. Liu, H.-Y. Chuang, H.-H. Tseng, T.-Y. Chen, C.-H. Chen, M.-S. Yu, Q. Li, A. Lueking, S.-H. Chen, Hydrogen Spillover Effect of Pt-Doped Activated Carbon Studied by Inelastic Neutron Scattering, The Journal of Physical Chemistry Letters, 2 (2011) 2322-2325.
[28] H. Yoshida, A. Yamamoto, S. Hosokawa, S. Yamazoe, S. Kikkawa, K. Hara, M. Nakamura, K. Kamazawa, T. Tanaka, Observation of Adsorbed Hydrogen Species on Supported Metal Catalysts by Inelastic Neutron Scattering, Topics in Catalysis, 64 (2021) 660-671.
[29] P.W. Albers, M. Lopez, G. Sextl, G. Jeske, S.F. Parker, Inelastic neutron scattering investigation on the site occupation of atomic hydrogen on platinum particles of different size, Journal of Catalysis, 223 (2004) 44-53.
[30] S.F. Parker, C.D. Frost, M. Telling, P. Albers, M. Lopez, K. Seitz, Characterisation of the adsorption sites of hydrogen on Pt/C fuel cell catalysts, Catalysis Today, 114 (2006) 418-421.
[31] M. Carosso, A. Lazzarini, A. Piovano, R. Pellegrini, S. Morandi, M. Manzoli, J.G. Vitillo, M.J. Ruiz, C. Lamberti, E. Groppo, Looking for the active hydrogen species in a 5 wt% Pt/C catalyst: a challenge for inelastic neutron scattering, Faraday Discussions, 208 (2018) 227-242.
[32] E. Vottero, M. Carosso, M. Jiménez-Ruiz, R. Pellegrini, E. Groppo, A. Piovano, How do the graphenic domains terminate in activated carbons and carbon-supported metal catalysts?, Carbon, 169 (2020) 357-369.
[33] A. Lazzarini, A. Piovano, R. Pellegrini, G. Leofanti, G. Agostini, S. Rudić, M.R. Chierotti, R. Gobetto, A. Battiato, G. Spoto, A. Zecchina, C. Lamberti, E. Groppo, A comprehensive approach to investigate the structural and surface properties of activated carbons and related Pd-based catalysts, Catalysis Science & Technology, 6 (2016) 4910-4922.
[34] A.L. Bugaev, A.A. Guda, K.A. Lomachenko, V.V. Shapovalov, A. Lazzarini, J.G. Vitillo, L.A. Bugaev, E. Groppo, R. Pellegrini, A.V. Soldatov, J.A. van Bokhoven, C. Lamberti, Core–Shell Structure of Palladium Hydride Nanoparticles Revealed by Combined X-ray Absorption Spectroscopy and X-ray Diffraction, The Journal of Physical Chemistry C, 121 (2017) 18202-18213.
[35] A.L. Bugaev, A.A. Guda, A. Lazzarini, K.A. Lomachenko, E. Groppo, R. Pellegrini, A. Piovano, H. Emerich, A.V. Soldatov, L.A. Bugaev, V.P. Dmitriev, J.A. van Bokhoven, C. Lamberti, In situ formation of hydrides and carbides in palladium catalyst: When XANES is better than EXAFS and XRD, Catalysis Today, 283 (2017) 119-126.
[36] G. Agostini, C. Lamberti, R. Pellegrini, G. Leofanti, F. Giannici, A. Longo, E. Groppo, Effect of Pre-Reduction on the Properties and the Catalytic Activity of Pd/Carbon Catalysts: A Comparison with Pd/Al2O3, ACS Catalysis, 4 (2014) 187-194.
[37] G. Agostini, E. Groppo, A. Piovano, R. Pellegrini, G. Leofanti, C. Lamberti, Preparation of Supported Pd Catalysts: From the Pd Precursor Solution to the Deposited Pd2+ Phase, Langmuir, 26 (2010) 11204-11211.
[38] R. Pellegrini, G. Leofanti, G. Agostini, E. Groppo, M. Rivallan, C. Lamberti, Pd-Supported Catalysts: Evolution of Support Porous Texture along Pd Deposition and Alkali-Metal Doping, Langmuir, 25 (2009) 6476-6485.

[39] K.M. Kaprielova, O.A. Yakovina, I.I. Ovchinnikov, S.V. Koscheev, A.S. Lisitsyn, Preparation of platinum-on-carbon catalysts via hydrolytic deposition: Factors influencing the deposition and catalytic properties, Applied Catalysis A: General, 449 (2012) 203-214.
[40] M. Jiménez-Ruiz, A. Ivanov, S. Fuard, LAGRANGE - the new neutron vibrational spectrometer at the ILL, Journal of Physics: Conference Series, 549 (2014) 012004.
[41] [Dataset], E. Vottero, M. Carosso, E. Groppo, M. Jimenez-Ruiz, C. Lamberti, R. Pellegrini, A. Piovano, Hydrides formation and spillover effect investigation on Pd-based catalysts (2019).
[42] [Dataset], A. Piovano, G. Agostini, M. Carosso , E. Groppo, M. Jimenez Ruiz, C. Lamberti, A. Lazzarini, M. Manzoli, S. Morandi, R. Pellegrini, E. Vottero, Study of the Pt-hydride formation and spillover effect on Pt/Al2O3 and Pt/C catalysts DOI:10.5291/ILL-DATA.7-05-466, 2016.
[43] P.W. Albers, J. Pietsch, J. Krauter, S.F. Parker, Investigations of activated carbon catalyst supports from different natural sources, Physical Chemistry Chemical Physics, 5 (2003) 1941-1949.
[44] P.W. Albers, W. Weber, K. Möbus, S.D. Wieland, S.F. Parker, Neutron scattering study of the terminating protons in the basic structural units of non-graphitising and graphitising carbons, Carbon, 109 (2016) 239-245.
[45] P.C.H. Mitchell, S.F. Parker, J. Tomkinson, D. Thompsett, Adsorbed states of dihydrogen on a carbon supported ruthenium catalyst Inelastic neutron scattering study, Journal of the Chemical Society, Faraday Transactions, 94 (1998) 1489-1493.
[46] P.A. Georgiev, D.K. Ross, A. De Monte, U. Montaretto-Marullo, R.A.H. Edwards, A.J. Ramirez-Cuesta, M.A. Adams, D. Colognesi, In situ inelastic neutron scattering studies of the rotational and translational dynamics of molecular hydrogen adsorbed in single-wall carbon nanotubes (SWNTs), Carbon, 43 (2005) 895-906.
[47] P.C.H. Mitchell, S.F. Parker, A.J. Ramirez-Cuesta, J. Tomkinson, Vibrational Spectroscopy with Neutrons, WORLD SCIENTIFIC2005.
[48] M. Sharpe, W.T. Shmayda, K. Glance, Measurement of Palladium Hydride and Palladium Deuteride Isotherms between 130 K and 393 K, Fusion Science and Technology, (2020) 642-648.
[49] E. Vottero, M. Carosso, A. Ricchebuono, M. Jiménez-Ruiz, R. Pellegrini, C. Chizallet, P. Raybaud, E. Groppo, A. Piovano, Evidence for H2-Induced Ductility in a Pt/Al2O3 Catalyst, ACS Catalysis, 12 (2022) 5979-5989.
[50] A.R. McInroy, D.T. Lundie, J.M. Winfield, C.C. Dudman, P. Jones, S.F. Parker, D. Lennon, The interaction of alumina with HCl: An infrared spectroscopy, temperature-programmed desorption and inelastic neutron scattering study, Catalysis Today, 114 (2006) 403-411.
[51] W. Karim, C. Spreafico, A. Kleibert, J. Gobrecht, J. VandeVondele, Y. Ekinci, J.A. van Bokhoven, Catalyst support effects on hydrogen spillover, Nature, 541 (2017) 68-71.
[52] D.K. Ross, V.E. Antonov, E.L. Bokhenkov, A.I. Kolesnikov, E.G. Ponyatovsky, J. Tomkinson, Strong anisotropy in the inelastic neutron scattering from PdH at high energy transfer, Physical Review B, 58 (1998) 2591-2595.
[53] T. Springer, D. Richter, 10. Hydrogen in Metals, in: D.L. Price, K. Sköld (Eds.) Methods in Experimental Physics, Academic Press1987, pp. 131-186.
[54] H. Conrad, M.E. Kordesch, R. Scala, W. Stenzel, Surface Resonances on Pd(111)/H Observed with HREELS, Studies in Surface Science and Catalysis, 26 (1986) 289-298.
[55] T.H. Ellis, M. Morin, The vibrational modes of hydrogen adsorbed on Pd(110), Surface Science Letters, 216 (1989) L351-L356.
[56] C. Nyberg, C.G. Tengstål, Vibrational Interaction between Hydrogen Atoms Adsorbed on Pd(100), Physical Review Letters, 50 (1983) 1680-1683.
[57] H. Conrad, M.E. Kordesch, W. Stenzel, M. Sunjić, B. Trninic-Radja, Surface resonances in vibrational spectroscopy of hydrogen on transition metal surfaces: Pd(100) and Pd(111), Surface Science, 178 (1986) 578-588.
[58] B. Lin, X. Wu, L. Xie, Y. Kang, H. Du, F. Kang, J. Li, L. Gan, Atomic Imaging of Subsurface Interstitial Hydrogen and Insights into Surface Reactivity of Palladium Hydrides, Angewandte Chemie International Edition, 59 (2020) 20348-20352.
[59] S. Villa-Cortés, R. Baquero, On the calculation of the inverse isotope effect in PdH(D): A Migdal-Eliashberg theory approach, Journal of Physics and Chemistry of Solids, 119 (2018) 80-84.

[60] H. Jobic, A. Renouprez, Formation of hydrides in small particles of palladium supported in Y-zeolite, Journal of the Less Common Metals, 129 (1987) 311-316.